2015-04-30

Circularly Polarized Solar Antenna for Airborne Communication Nodes

Oisin O'Conchubhair
Dublin Institute of Technology, oisin.oconchubhair@mydit.ie

Adam Narbudowicz
Dublin Institute of Technology, adam.narbudowicz@dit.ie

Patrick McEvoy
Dublin Institute of Technology, patrick.mcevoy@dit.ie

Max Ammann
Dublin Institute of Technology, max.ammann@dit.ie

Recommended Citation

O'Conchubhair, O.; Narbudowicz, A.; McEvoy, P.; Ammann, M.J., "Circularly polarised solar antenna for airborne communication nodes" *Electronics Letters* , vol.51, no.9, pp.667,669, 4 30 2015 doi:10.1049/el.2015.0201

Circularly Polarized Solar Antenna for Airborne Communication Nodes

Oisin O'Conchubhair, Adam Narbudowicz, Patrick McEvoy and Max J. Ammann

A circularly polarized solar cell antenna consisting of four sequentially rotated printed inverted-F antennas is proposed. Four multicrystalline silicon solar cells act as the ground plane and the antenna is suitable for low power airborne communication nodes and wireless sensor networks. The antenna design was developed to allow 100% insolation of the cells when directly facing a light source. The low-profile antenna minimises shadowing of the solar cell for oblique angle insolation.

Introduction: Low-altitude airborne communication nodes are envisaged for improved wireless communications over remote areas and to support emergency services responding to large scale natural disasters [1]. Short-term systems can be deployed rapidly to the lower troposphere, while longer-term systems are placed in the upper troposphere or stratosphere. Networked nodes are to communicate with each other and with ground users. Entirely solar powered, each node makes use of increased solar energy availability at altitude to charge lithium batteries for low light conditions [2]. TETRA, WiFi and WiMAX radios have been tested on tethered balloons [3], with TETRA achieving 9 km but with WiFi achieving higher data rates at 1 km. The proliferation of WiFi enabled consumer devices also makes it a viable aid in emergency situations. Airborne antenna orientation can be widely variable, so circular-polarisation (CP) is considered due to reduced polarization mismatch losses.

Most work to date has focused on antenna designs which have potential for solar integration. With an aim to integrate a CP antenna with a small satellite solar panel, two linearly-polarized meshed patch antennas were prototyped using a substitute Rogers laminate [4]. While a 5.15 dBi gain at 2.47 GHz was achieved, it expected that a lossy solar cell substrate would degrade the gain performance. The 2% S11 bandwidth covers WiFi channels 9-14. The CP bandwidth of 0.61% has 3-dB beamwidths of 20° and 80° in the principle planes.

Only one paper presents the integration of CP antennas with solar cells. A 3.87 GHz amorphous silicon solar cell was prototyped with an integrated crossed-slot antenna [5]. The slot was excited by a microstrip line beneath the slot. A 3.7 dBi gain was achieved using a reflector 10 mm behind the feed line, with a 10.8 mm overall device thickness. The antenna achieves a 3.1% CP bandwidth that covers the 2.6% impedance bandwidth. The beamwidths were 46° and 71° in the principle broadside planes.

This paper presents the integration of four low-profile printed inverted-F antennas (IFAs) with four multicrystalline solar cells suited to airborne CP communications. The antennas are sandwiched between neighbouring solar cells to minimise the profile and solar shadowing. The antenna is designed to achieve CP over the WLAN channels 2.4 - 2.45 GHz. The solar panels on a high altitude aerial balloon are mounted almost perpendicular to the earth's surface ensuring optimal solar cell insolation during shorter winter days [1]. Mounting the IFAs between the solar cells in these panels provides ideal antenna orientation for communication between aerial nodes.

Proposed Antenna Configurations: Four multicrystalline solar cells are arranged to form a square ground plane for the 322 mm wide antenna over a lightweight support. Each solar cell has a length and width of 156 mm and consists of three elements, a latticed anode front contact, an aluminium rear contact cathode layer and a multicrystalline silicon material between the contacts. The 0.1 mm wire lattice layout allows the maximum insolation of the semiconductor material while maintaining an adequate surface contact to yield the maximum power output. Two perpendicularly oriented 2 mm wide bus-bars, 74.18 mm apart, interconnect the 57 electrode wires.

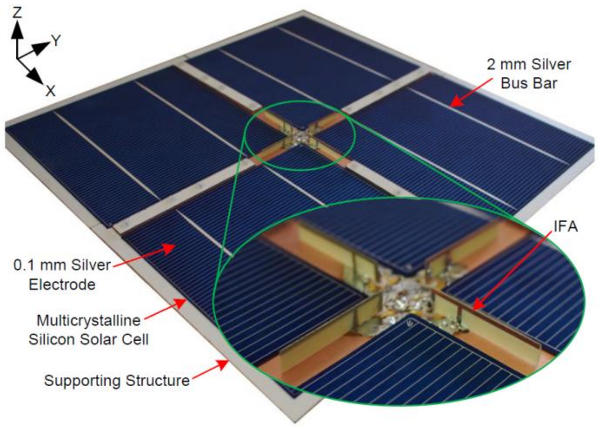

Fig. 1 *CP solar antenna configuration*

The antenna uses the cathode layer beneath the solar cells instead of a metal ground plane thus reducing the aerial vehicle weight. A copper strip connects the rear contacts of each high power cell providing an output of over 12 W, considerably more than a-Si alternatives [5]. The arrangement is shown in Fig. 1.

The IFA dimensions are $H_A = 6$ mm, $T_A = 1$ mm, $L_A = 22.65$ mm, $L_C = 8.67$ mm and $L_S = 8.96$ mm, shown in Fig. 2. Each antenna is positioned between a pair of solar cells without the need for expensive customised cells. This location allows for 100% insolation of the cell when directly facing a light source, with 30% less shadowing than the meshed patch [4]. While the low-profile of the antenna minimises shadow casting from light sources at low oblique angles, this has lower impact than the loss of light intensity at low angles.

A rat race coupler and two branchline couplers are employed to provide sequentially rotated phases for CP. The simulations were carried out using CST Microwave Studio. Identical antennas positioned above a copper ground plane and fed using the same transmission line configuration were simulated for comparison.

Results and Discussion: The feed line network has measured insertion losses of -6.9 dB, -6.6 dB, -6.8 dB and -6.5 dB from ports 2, 3, 4 and 5, respectively. The measured phase offset between ports 2 and 3 was 89.5º, between ports 3 and 4 was 90.0º, between ports 4 and 5 was 89.7º and between ports 5 and 2 was 90.9º.

The simulated and measured results for each antenna are given in Table I. The simulated and measured S11 for each antenna is shown in Fig. 3 and isolation is shown in Fig. 4. The measured bandwidth was slightly less than simulated by 0.3 percentage points due to manufacturing discrepancies in the assembly of the four antennas and the solar panel.

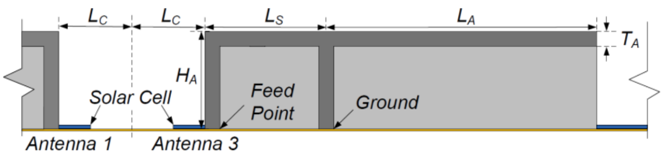

Fig. 2 *Printed inverted-F antenna parameters*

Table 1: Integrated Element Results

	Frequency (GHz)	-10dB Bandwidth (%)
Simulated Solar Antenna 1	2.45	1.7
Measured Solar Antenna 1	2.45	1.6
Simulated Solar Antenna 2	2.46	1.8
Measured Solar Antenna 2	2.45	1.5
Simulated Solar Antenna 3	2.45	1.7
Measured Solar Antenna 3	2.45	1.5
Simulated Solar Antenna 4	2.46	1.8
Measured Solar Antenna 4	2.45	1.6
Simulated Copper Antenna	2.42	1.7

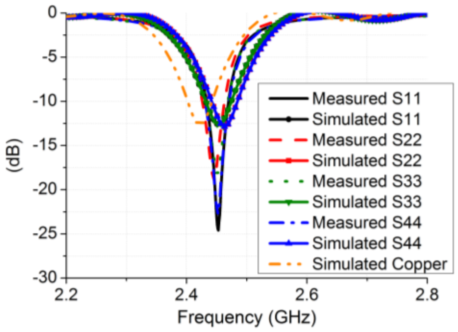

Fig. 3 *Measured and simulated S11 for each antenna*

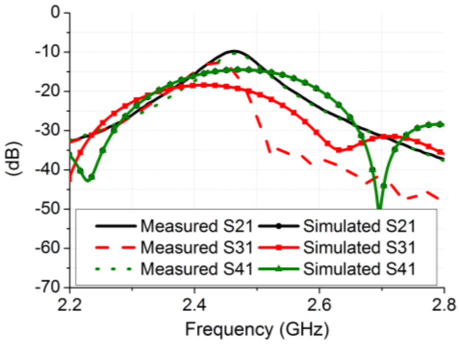

Fig. 4 *Measured and simulated isolation between antennas*

When comparing a simulated setup using a solid copper ground plane instead of multicrystalline silicon, the wider bandwidth is attributed to losses in the silicon. Bandwidths can be further increased with higher antennas. In addition, the is resonance is slightly higher in the solar case due to an electrical shortening of the antenna, where the silicon surface is proud compared to the copper surface.

Simulated and measured isolation between antennas is better than 10 dB in all cases for 2.4 - 2.45 GHz. The simulated axial-ratio is below 3 dB for 2.33 - 2.58 GHz. The measured axial-ratio is below 3 dB for 2.29 - 2.63 GHz. Axial-ratio results are shown in Fig. 5.

The feed line is configured for left hand circular polarization (LHCP), shown in Fig. 6. Measured LHCP gain for the solar antenna is 3.7 dBic at boresight while RHCP gain is -10.2 dBic. Gain results are shown in Table II and no significant degradation in radiation properties of the solar antenna is observed compared to the copper case. The measured beamwidth for the solar antenna was 51° and 58° in the XZ and YZ planes respectively. Radiation patterns are shown in Fig. 6. The antenna can be re-configured for RHCP, linear polarizations and beam switching by changing the phase arrangement. Linear polarizations are achieved by feeding two opposing elements in the array; simulations show the antenna beamwidth to be 114° in the plane of the inactive elements and 51° in the plane of the active elements.

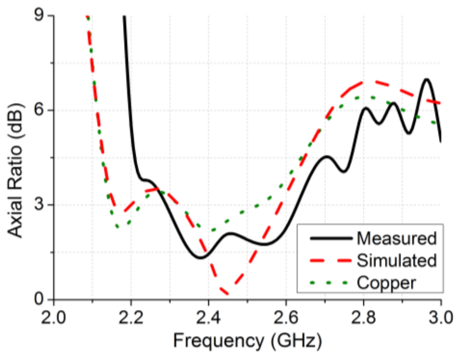

Fig. 5 *Measured and simulated axial ratio*

TABLE II: Antenna Radiation Results at 2.45 GHz

Antenna	LHCP Boresight Gain (dBic)	RHCP Boresight Gain (dBic)	Axial Ratio Bandwidth (%)	LHCP Beamwidth (°)	
				X-Z	Y-Z
Meas Solar	3.7	-10.2	13.8	51	58
Sim Solar	4.0	-13.5	10.4	61	61
Sim Cu	4.0	-12.7	8.3	61	61

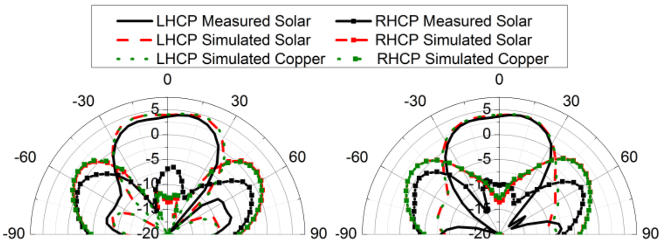

Fig. 6 *CP Gain X-Z (left) and Y-Z (right)*

Conclusion: The first integration of sequentially rotated IFA antennas with a high power photovoltaic solar panel is reported. Locating the antennas between solar cells in a 12 W solar panel results in greater power generation than previous solar CP designs and avoids costly customised solar cells [5]. The configuration ensures 100% solar cell insolation when directly facing light sources, while the low-profile minimises shadowing due to oblique angle light sources.

Beam switching and polarization reconfiguration can be achieved by adjusting the phase between antenna elements, allowing the antenna to cover a larger area than other CP integrations.

Acknowledgments: This work was part funded by the Irish Higher Education Authority under PRTLI Cycle 5 as part of the Telecommunication Graduate Initiative and by Science Foundation Ireland grant number 13/TIDA/I2746.

O. O'Conchubhair, A. Narbudowicz, P. McEvoy and M.J. Ammann (*Antenna & High Frequency Research Centre, School of Electrical and Electronic Engineering, Dublin Institute of Technology, Dublin, Ireland*)

E-mail: oisin.oconchubhair@mydit.ie

References

1. "Project Loon", http://www.google.com, [online]. Available: http://www.google.com/loon/ [Accessed Dec. 12, 2014].
2. "Prospects for Commercial Stratospheric Industrialisation at the Threshold of Space", athenalab.com, Oct. 16, 2010. [online]. Available: http://www.athenalab.com/Prospects_for_commercial_stratospheric_industrialization.pdf . [Accessed Dec. 15, 2014].
3. A. Vilhar, A. Hrovat, T. Javornik, M. Mohorčič, "Experimental Analysis of Wireless Temporary Networks Deployed by Low Altitude Platforms" *IEEE 18th International Workshop on Computer Aided Modelling and Design of Communication Links and Networks* (CAMAD), 2013, pp. 238-242.
4. T. Yasin, R. Baktur, "Circularly Polarized Meshed Patch Antenna for Small Satellite Application," *IEEE Antennas and Wireless Propagat. Lett.*, 12, pp. 1057-1060, 2013.
5. S. Vaccaro, J.R. Mosig, P. de Maagt, "Two advanced solar antenna "SOLANT" designs for satellite and terrestrial communications," *IEEE Trans on Antennas and Propagat.* 51, (8), pp. 2028-2034, 2003.